Biosensors and Bioelectronics 205 (2022) 114128

Contents lists available at ScienceDirect

Biosensors and Bioelectronics

journal homepage: www.elsevier.com/locate/bios

A sweat-activated, wearable microbial fuel cell for long-term, on-demand power generation

Jihyun Ryu [a], Mya Landers [a], Seokheun Choi [a,b,*]

[a] Bioelectronics & Microsystems Laboratory, Department of Electrical & Computer Engineering, State University of New York at Binghamton, Binghamton, NY, 13902, USA

[b] Center for Research in Advanced Sensing Technologies & Environmental Sustainability, State University of New York at Binghamton, Binghamton, NY, 13902, USA

ARTICLE INFO

Keywords:
Wearable microbial fuel cells
Sweat-based power generation
Bacillus subtilis
Sporulation
And germination

ABSTRACT

In this work, we enabled on-demand, long-functioning, sweat-based power generation through a wearable paper-based microbial fuel cell (MFC) using a novel spore-forming biocatalyst, *Bacillus subtilis*. The MFC is sustainable and survivable even in the extreme environmental conditions of human skin. *B. subtilis*, usually found on the skin, was able to form endospores that endure extreme dryness or nutrient limitation when sweat access was limited or unpredictable for humans at rest, offering long-term operation and stable storage. When human sweat was introduced, spore germination and gradual power generation were observed without adding nutrient germinants. Through repeated sporulation and germination depending on the sweat availability, *B. subtilis* provided a sustainable solution for an innovative sweat-activated power source that can result in the long-lasting vision of self-sustaining wearable electronics. Even after the 48-h operation, the device generated a maximum power density of 24 $\mu W/cm^2$ and a maximum current density of 175 $\mu A/cm^2$, which is comparable to or even higher than the previously reported paper-based MFCs using well-known strong exoelectrogens in an optimized bacterial medium. Furthermore, *B. subtilis* in sweat was shown to be commensal with other skin microorganisms while producing antibiotic substances that were effective against potential pathogens, exhibiting a great potential for seamless and intimate integration with skin-mountable applications.

1. Introduction

The past two decades have witnessed significant developments and performance improvements in wearable electronics (Niu et al., 2020; Yang and Gao, 2019). Among various physiological signals generated from the human body, biomarkers available in sweat have recently received considerable attention as meaningful information that can be readily collected non-invasively and accessed continuously through skin-mountable wearable technologies (Barlya et al., 2018; Ghaffari et al., 2021a,b; Hernandez-Rodriguez et al., 2021). These sweat-based wearable electronics can provide real-time diagnostics and immediately actionable healthcare information, enabling timely access to early treatment. Many pharmacological agents and iontophoresis have been used to trigger the excretion of sweat even at rest, thereby allowing continuous sweat monitoring (Choi et al., 2018). However, the sweating rate and total sweat volume are very correlated with metabolic activity of the human body and reflect underlying health conditions. Therefore, long-term measurement of variable sweat dynamics is becoming a requirement for wearable sweat sensors (Baker, 2017; Ghaffari et al., 2021a,b). Furthermore, the innovative micro- and nano-fluidic wearable techniques, which enabled the collection of an extremely small volume of resting thermoregulatory sweat (Nyein et al., 2021; Zhao et al., 2020), demand continuous and long-lasting operation and require reliable sources of power (Manjakkal et al., 2021; Yeon et al., 2021). Unfortunately, enzymatic fuel cells, which have been considered as the dominant sweat-based power source for wearable electronics (Wu et al., 2021; Jeerapan et al., 2020), cannot provide reliable, long-lived power generation because many oxidation-reduction enzymes readily and quickly degenerate under non-optimal ambient conditions, thus reducing their biocatalytic reactions, stability and shelf life, and power (Xiao et al., 2019; Rasmussen et al., 2016). Moreover, the active redox centers are inserted deeply inside the enzyme matrix, which decrease the electron transfer efficiency from the enzyme active site to the electrodes (Osman et al., 2011). Many studies have developed innovative

* Corresponding author. Bioelectronics & Microsystems Laboratory, Department of Electrical & Computer Engineering, State University of New York at Binghamton, Binghamton, NY, 13902, USA.
E-mail address: sechoi@binghamton.edu (S. Choi).

https://doi.org/10.1016/j.bios.2022.114128
Received 14 February 2022; Received in revised form 21 February 2022; Accepted 22 February 2022
Available online 25 February 2022

techniques to address these issues such as novel immobilization methods, addition of exogenous electron mediators, creation of direct electron transfer pathways, and integration with energy storing devices (Xiao et al., 2019; Rasmussen et al., 2016; Osman et al., 2011; Ivanov et al., 2010). However, fundamental breakthroughs are required for enzymatic fuel cells to acquire a long-lasting, self-sustaining, practical power solution for wearable applications.

On the other hand, energy harvesting techniques using microorganisms are considerably more robust than the enzymatic methods and offer greater self-sustaining characteristics with long-time stability (Osman et al., 2010, 2011). In particular, bacteria in microbial fuel cells (MFCs) include entire enzymatic pathways and reproduce biocatalytic enzymes through their natural metabolism (Osman et al., 2010). Furthermore, there are many naturally occurring electrogenic bacteria with a direct electron transfer mechanism, and various simple but low-cost approaches are available to readily promote extracellular electron transfer even in weak electrogenic bacteria (Chen et al., 2019; Kumar et al., 2017). Given that sweat contains valuable nutrients necessary for bacteria and a wide range of microorganisms are colonized on the skin (Byrd et al., 2018; Brandwein et al., 2016), microbial energy harvesting is a most attractive power solution that can enable long-lived wearable electronics. However, microbial power generation has barely been explored mainly because of a potential risk of bacterial infection and the low survival rate of bacteria on the skin, which has harsh environmental conditions. Recently, our research group discovered that three Gram-positive, skin-inhabiting bacteria, *Staphylococcus epidermidis*, *Staphylococcus capitis*, and *Micrococcus luteus*, possessed obvious electrogenic capabilities that are comparable to those of the well-known Gram-negative exoelectrogen, *Shewanella oneidensis* (Mohammadifar et al., 2020). The discovery opens the possibility that other Gram-positive skin bacteria have electrogenic capabilities. Using the human skin bacteria extracted from and applied directly to the host was expected to minimize foreign-body response. However, it was challenging to maintain bacterial viability and balance their populations with other skin microorganisms in sweat that contains antimicrobial substances. Even our latest wearable MFCs with skin bacteria were limited to a very short operation time for one-time use. Furthermore, with the irregular perspiration on the skin in combination with evaporation, an optimal nutrient-rich environment was not continuously provided for long-term bacterial growth and survival.

In this work, we, *for the first time*, developed a long-lasting wearable MFC by using a spore-forming skin bacterium, *Bacillus subtilis*, which can use its adaptive strategy to survive in harsh environmental conditions. *B. subtilis* is one of the most frequently found species in neonates and is predominately located in the plantar skin of healthy adults (Hernandez-Valdes et al., 2020). Because *B. subtilis* is a Gram-positive bacterium with a very thick cell membrane, its electrogenicity has been reported to be very weak and has not been considered as suitable biocatalysts for power generation and wastewater treatment in macro-sized MFC platforms (Logan et al., 2019). However, as our preliminary report had demonstrated, the electrogenic capability of *B. subtilis* is sufficient for small-scale battery-reliant applications such as wearable electronics (Ryu and Choi, 2021). Furthermore, the natural ability of *B. subtilis* to form very resistant dormant endospores in response to extreme environmental stresses allows it to serve as a dormant biocatalyst for the MFC. The dormancy of *B. subtilis* preserves the bacteria for a long period of time without denaturation or degradation. Additional chemical germinants had activated the spore germination, allowing the MFC to achieve a high-power density of 16.6 $\mu W/cm^2$ (Ryu and Choi, 2021). Three serially connected devices produced enough electricity to power an electrical calculator. That preliminary result provided a foundation for the development of a fully self-sustaining, long-lived MFC with repeated sporulation and germination while avoiding the use of additional nutritious germinants that hamper self-sustaining, stand-alone operation. The three-part central hypothesis of this work is that (i) the bacterial sporulation and germination can be repeatedly performed depending on the sweat availability, (ii) human sweat includes potential germinants to initiate the spore germination, and (iii) *B. subtilis* can perform commensal or competitive interactions with other skin microorganisms to maintain the composition of our skin microbiota in a densely populated but harsh skin environment. This work demonstrates how the sweat availability affected long-term electricity generation from *B. subtilis* while they transition into a dormant state as spores or returning to life in the process of germination (Fig. 1a & b). The bacterial power generation was measured in the paper-based MFC while we delivered sweat samples through an integrated sweat simulator. Paper offers many exciting opportunities for sweat-based wearable electronics because of its unique features such as capillary-driven microfluidic behavior, biocompatibility, flexibility, low cost, and biodegradability (Xu et al., 2021). Our group created paper-based MFCs and initiated the field of paper-based power sources (Gao et al., 2019; Gao and Choi, 2018; Mohammadifar et al., 2018). Our recent technique for the paper-based MFC was innovatively leveraged for wearable applications. Because *B. subtilis* can protect the skin by producing antibiotics, our wearable paper-based MFC will be a more suitable power source for existing wound-healing devices or drug delivery systems (Fig. 1c). Furthermore, the paper-based MFC using *B. subtilis* can create opportunities for the design of innovative bacteria-powered sensing devices to monitor human skin health. Depending on the individuals' dietary habits or health conditions, the sweat constituents will vary and affect the metabolism of *B. subtilis*, changing the electricity generation (Fig. 1d) (Baker, 2017; Ghaffari et al., 2021a,b).

2. Results and discussion

2.1 *B. subtilis* sporulation and germination in sweat. On-demand power generation produced only when natural perspiration occurs will support wearable electronics with sensors that can analyze sweat's properties. When sweat secretion stops, the electronics must enter into standby mode to conserve power. In this sense, *B. subtilis* can become an ideal biocatalyst in a wearable MFC for sweat-activated on-demand

Fig. 1. Conceptual image for the task impact. (a & b) The use of *B. subtilis* as a biocatalyst for the MFC will offer greater self-sustainability with long-term stability and shelf life for wearable applications. (c) Antibiotics produced from the bacteria will inhibit the infections of other pathogens. (d) Bacterial electrogenicity will be used as a biosensing mechanism as it is sensitively changed according to the sweat dynamics and constituents.

power generation. In harsh environmental conditions such as nutrition depletion or dryness because of lack of sweat, *B. subtilis* can transition into a dormant state as its spores have multiple protective layers to tolerate those external stresses, ensuring their long-term survival and viability (Khanna et al., 2020). When nutrient-rich sweat is available, bacterial germination readily activates (Christie and Setlow, 2020), harvesting metabolic-produced electricity by oxidizing biodegradable substrates in sweat. The challenging part is that the bacterial spores respond mainly to specific germinants, such as L-alanine, L-valine, and L-asparagine, in the environment to revive (Christie and Setlow, 2020; Sayer et al., 2019). Their germination process with anything other than those specific nutrients has not been well-understood, particularly not in human sweat. If the wearable MFC requires the repeated introduction of those germinants to trigger spore germination, power autonomy and sustainability cannot be realized because continual intervention is necessary.

As shown in Fig. 2a, we kept track of the spore germination process with continual sweat introduction by assessing the transition of spores from phase-bright to phase-dark (Kong et al., 2011). The phase-contrast imaging has been widely used to easily identify the spore revival in the early stage of germination, as the water uptake first happens during spore germination, decreasing the refractive index of the spores. As a result, the germinating spores are phase-dark while the dormant spores appear phase-bright. The spores prepared by nutrient exhaustion triggered the germination immediately after the sweat was introduced (Figs. 2a–0 h). At 5 h, about 20% of the dormant spores became phase dark while germinating, followed by a greater number of germinated cells through 60 h (Figs. 2a–5 h and 60 h). Although further studies are needed to find what potential germinants are available in sweat and what mechanism of signal transduction initiates germination, notably spore germination was triggered by human sweat.

As shown in Fig. 2b, *B. subtilis* in sweat-depleted nutrients induce sporulation. Cells were grown for 24 h until the exponential phase, and then sporulation was gradually initiated over 150 h as nutrients were depleted. The culture contained more than 98% of phase-bright spores. While many nutrients available in sweat may delay sporulation, a small amount of iron in sweat could induce rapid sporulation (Purohit et al., 2010). A faster and more homogeneous entry of the bacterial cells into the sporulation will be required for actual on-demand wearable applications. The spore-forming capability of *B. subtilis* in sweat can be a critical attribute that allows long-term survival without nutrients when humans cannot sweat. Usually, sweat evaporates quickly from the skin, possibly posing transient drought stress to *B. subtilis*. In that case, the cells initiated only partial sporulation to withstand the abrupt environmental change, instead of going through the energy-intensive transition into dormant endospores as they do for prolonged nutrient starvation (Gray et al., 2019). This result was in good agreement with previous studies showing that bacteria can slow growth substantially as an alternative strategy. They form non-dormant spores and enter a so-called "zombie mode" to survive some transient environmental stresses (Nield, 2019). As shown in Fig. 2c, with a dried condition after the sweat introduction stopped, the cells formed the coccoid-shaped

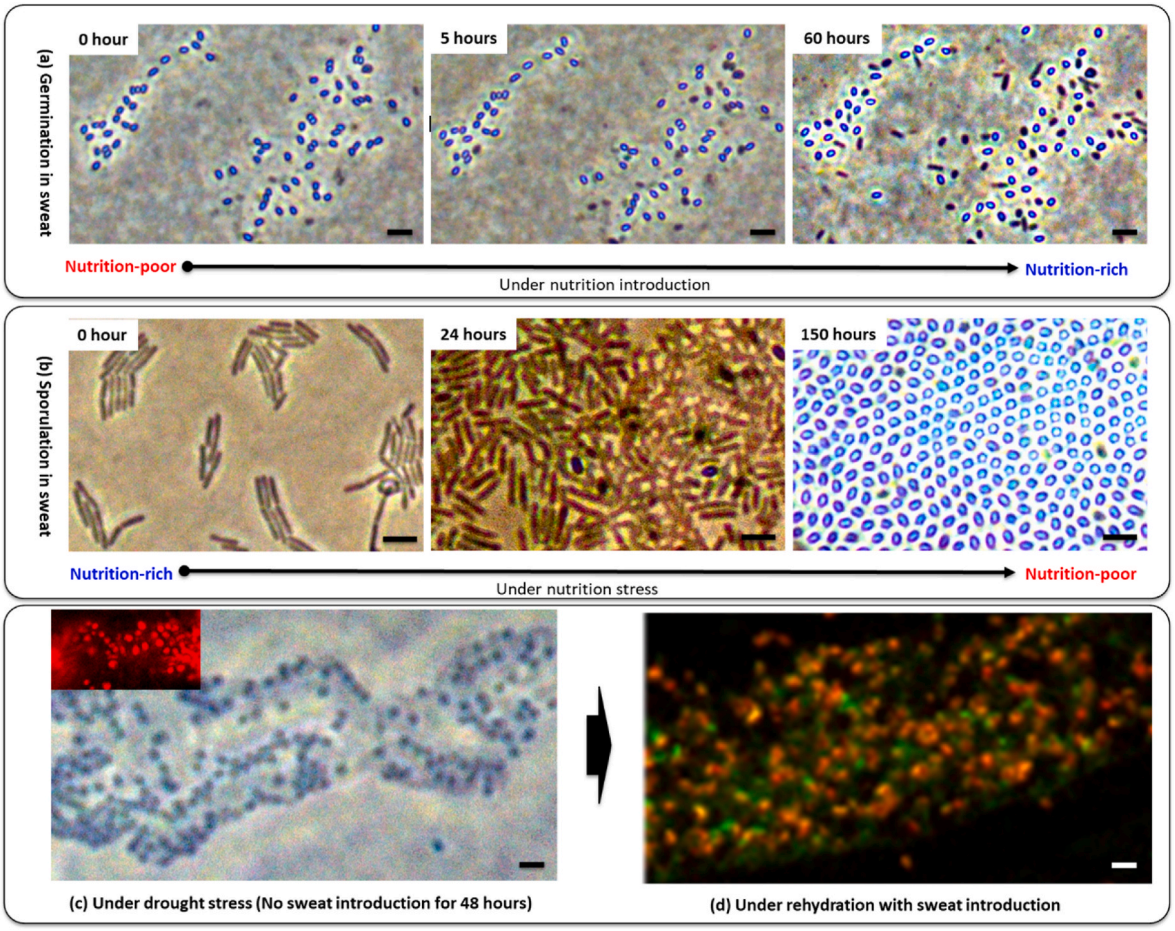

Fig. 2. Phase-contrast and fluorescent microsopic images of *B. subtilits* sporulation and germination. (a) Time-lapse phase-contrast images of the spore revival process with continous introduction of nutrient-rich sweat, (b) time-lapse phase-contrast images of the cells in sporulation induced by nutrient exhausion in sweat, (c) phase-contrast image of the spores induced by drought stress without sweat introduction for 48 h (subset: fluorescent image of the spores), and (d) fluorescent image of the spores after germination induction with sweat introduction (Scale bars: 10 μm).

spores, but they appeared phase-dark, indicating they are in the stage of germination with the water uptake. When we used a combination of two dyes with carboxy-fluorescein diacetate (cFDA) and propidium iodide (PI) to determine the morphological status of the cells, the spores were stained only with red PI fluorescence dye. The phase-contrast and fluorescent images show that the spores are neither dormant nor metabolically functioning. When sweat was re-introduced, the spores gradually became metabolically active, which becomes apparent with the addition of cFDA dye (Fig. 2d). Given that human skin frequently becomes dry with transient nutrient limitation because of sweat evaporation, the cellular transition into "zombie mode" under short-term drought stress and revival into "active mode" for metabolic growth can be an outstanding and unique merit process to exploit for sweat-based power generation.

2.1. On-demand power generation with in vitro perspiration

As a clinical and preclinical biocompatibility testing of *B. subtilis* has not been done yet in our group, *in vivo* studies with human subjects could not be performed. Alternatively, we characterized the power generation by providing real human sweat samples taken from three healthy volunteers using a syringe pump through an integrated sweat simulator and a microfluidic interface (Fig. S1). More details of the sweat simulator and its operation are found in our previous report (Mohammadifar et al., 2020). The wearable MFC was built on flexible paper substrates (Fig. 3). The MFC covered with 3M Tegaderm medical film provided tight adhesion with the heel's skin and effectively absorbed the sweat. We previously created many paper-based MFCs for disposable and wearable applications (Mohammadifar et al., 2020; Gao et al., 2019; Gao and Choi, 2018), which were effectively leveraged for sweat-based power generation especially with *B. subtilis*. The paper MFC was constructed on double sheets of Whatman 3 MM chromatography paper (for the anodic and cathodic layers) with an ~6 μm pore size so that any morphological forms of *B. subtilis* can be effectively stored (Germinated rod-shaped cells: 2–6 μm long and less than 1 μm in diameter, and spherical spores: ~1 μm in diameter). Because the bacterial cells are tightly attached to the cellulose paper fibers and a further packaging paper with a small pore size can be readily attached, a potential risk of bacteria leakage will be minimized. The anodic layer in which the bacterial cells would be inoculated was conductively engineered with a poly(3, 4-ethylenedioxythiophene):polystyrene sulfonate (PEDOT:PSS) to maximize the extracellular electron transfer from the bacteria. The redox polymer, PEDOT:PSS, can indirectly mediate bacterial extracellular electron transfer (Tahernia et al., 2020b). The cathodic layer was prepared with a solid-state Ag_2O catalyst for the reduction and a wax-based membrane to separate the cathode from the anode when assembled. In the assembled MFC, germinated *B. subtilis* can oxidize the available sweat, producing electrons and protons. The electrons move from the anode to the cathode through an external circuit while the protons diffuse to the cathode through the wax-based membrane. At the cathode, the electrons and the protons that traveled from the anode reduce Ag_2O to Ag. When the nutrients are not available in sweat because of evaporation and depletion, *B. subtilis* stops metabolizing and ends electron generation by transitioning into spores.

To characterize the electrogenicity of *B. subtilis* with *in vitro* perspiration, the spores were inoculated in the MFC and an external resistor

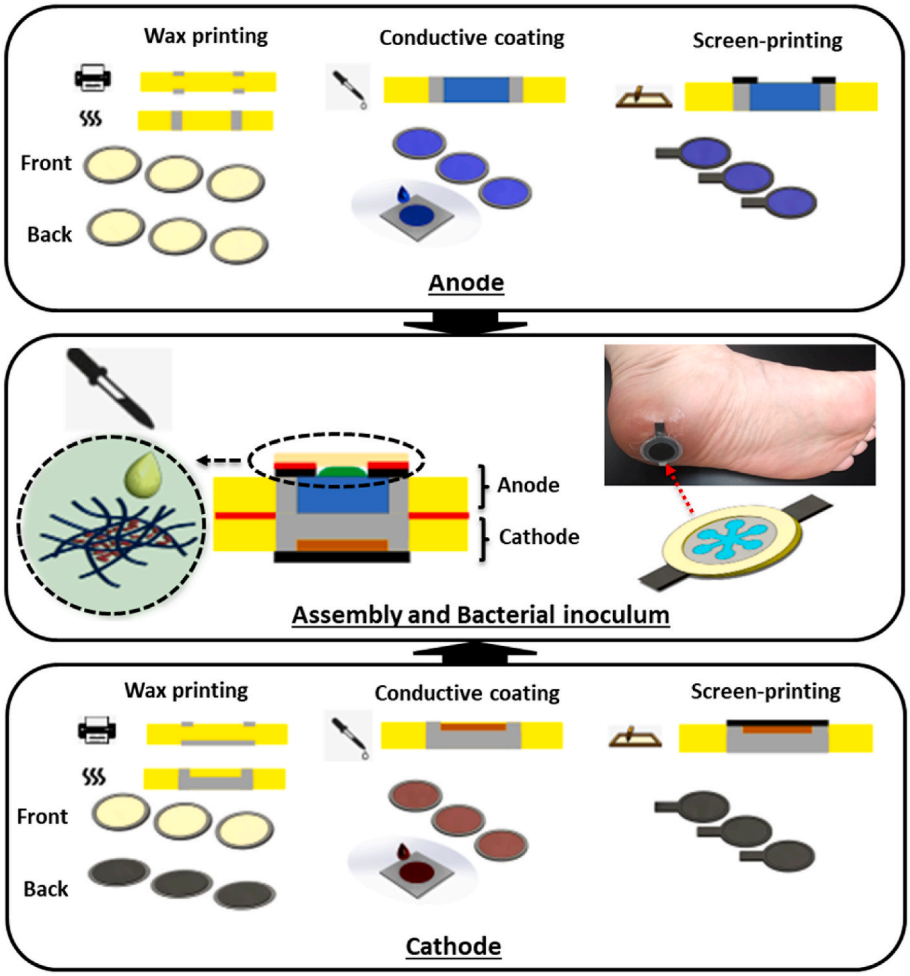

Fig. 3. Fabrication processes of a wearable paper-based MFC. The anode and the cathode were individually prepared and assembled together, followed by the introduction of *B. subtilis*. As a clinical and preclinical biocompatibility testing of *B. subtilis* has not been done yet in our group, *in vivo* studies with human subjects could not be performed. Alternatively, we characterized the power generation by providing real human sweat samples taken from three healthy volunteers. The MFC covered with 3M Tegaderm medical film provided tight adhesion with the foot skin and effectively absorbed the sweat.

(2.2 kΩ) was connected the anode and the cathode to allow the flow of electricity generated from the bacterial metabolism. To evaluate the performance of the *B. subtilis* MFC, two control groups were prepared; one without bacteria (Fig. 4a), and one with the well-known exoelectrogen, *S. oneidensis*, (Fig. 4b). Human sweat was introduced to all three MFC devices through the sweat simulator at a constant flow rate of 50 μL/h. Initially, all devices generated instantaneous peak power because the paper-based MFCs quickly absorbed the liquid through capillary action and the sudden chemical reactions of the ionic components in sweat with the electrodes generated an abiotic current. The MFC without bacteria generated ~ 7 μW/cm^2 of the abiotic power for about 4 h and then dropped abruptly to zero (Fig. 4a). The MFC inoculated with *S. oneidensis* generated slightly greater and longer power than the abiotic control (Fig. 4b). Its transient power was also higher for a longer period as the microbial power generation added to the abiotic one. However, the microbial metabolism and the subsequent electricity generation from *S. oneidensis* did not last for more than 7 h even in nutrient-rich sweat. This is presumably because human sweat contains highly efficient antibiotics, lowering the metabolism and viability of *S. oneidensis*. On the other hand, the MFC with *B. subtilis* demonstrated a quite interesting phenomenon having a gradual increase in power generation for 30 h and sustained the level (~10 μW/cm^2 at 2.2 kΩ) for another 25 h. This seems to be corelated with the spore gemination in sweat (Fig. 2a). In particular, *B. subtilis* dormant spores germinated much more rapidly (within 30 h) in this paper-based environment than the standard culture platform (Fig. 2a) where many cells remained as spores even at 60 h. This is mainly because the 3-D paper-based environment allows the microorganism to respond more effectively to a variety of chemical and physical cues and better perform the fundamental cellular activities than the 2-D culture technique (Tahernia et al., 2020a, 2020b). For more practical use, further study will be necessary to improve the germination speed. Alternatively, the MFC can be integrated with other energy-storage devices so that the excessive energy harvested from the sweat can be charged and discharged by the integrated energy-storage device during the relatively slow germination process (Liu et al., 2021)

Notably, the transient power value and duration of *B. subtilis* were much greater than the other two controls. Given that the spores are not metabolically active in this early gemination stage, the highest and longest peak value is hard to explain, but many enzymes available on the spore surface may react with the anodic surface of the MFC and generate more power (Zhang et al., 2020; Pan et al., 2012). At 55 h of operation, we stopped the flow of sweat into the device for 48 h. Surprisingly, the MFC power suddenly dropped to zero, which was maintained for 48 h. The cessation of power production can be well described with the experiment shown in Fig. 2c and d. The cells entered the dormant or "zombie" mode under the sudden nutrient depletion and evaporation. When the sweat introduction resumed, significant power was produced following the initial transient period. At this point, the polarization curve and power output of the MFC were measured as a function of the current. The device generated a maximum power density of 24 μW/cm^2 and a maximum current density of 175 μA/cm^2, which is comparable to or even higher than the previously reported paper-based MFCs using well-known strong exoelectrogens in an optimized bacterial medium (Gao and Choi, 2017, 2018; Mohammadifar et al., 2018; Mohammadifar and Choi, 2017). With other sweat samples taken from the other volunteers, the MFC demonstrated similar behaviours and comparable outputs (Fig. S2). However, with the replenishment of sweat after this 48-h dehydration, the decreasing power generation was observed and the MFC required some time to produce the original power output (data not shown).

2.2. Commensal and competitive interactions of B. subtilis with skin microorganisms

Our human skin, on which the wearable electronics are intimately mounted, harbors millions of bacteria that play a critical role in

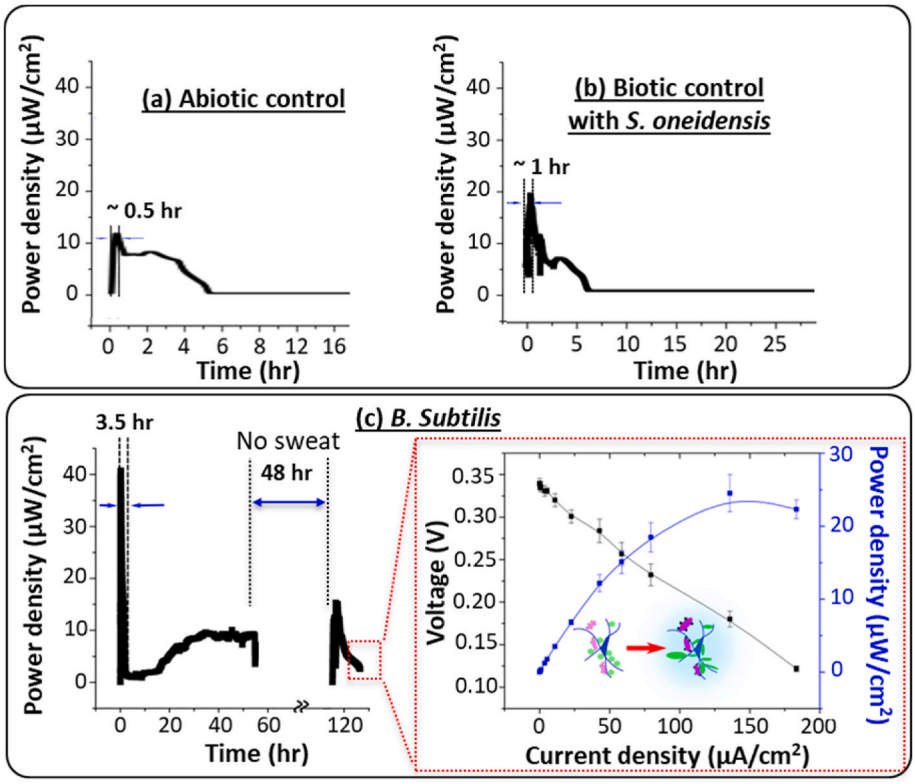

Fig. 4. Electrical performance characterization with *in vitro* sweat introduction. (a) abiotic control without bacteria, (b) biotic control with *Shewanel oneidensis*, and (c) *B. subtilis* under continuous sweat introduction with 48-h pause. Continous power measurement and polarization curve/power output of the MFC after the sweat introduction resumed.

inhibiting other pathogenic colonization and educating our immune system (Byrd et al., 2018; Brandwein et al., 2016). Although the composition of the microbial communities varies at different sites, their temporal stability becomes outstanding by balancing the bacteria communities and viabilities even with constant exposure to a changing external environment (Oh et al., 2016). Therefore, the use of foreign bacteria for wearable electronics can break this balance, causing skin disorders. *B. subtilis* was carefully chosen as a biocatalyst for this wearable MFC application. As *B. subtilis* can endure extreme skin environmental conditions, they frequently colonize normal human skin (Hernandez-Valdes et al., 2020). As shown in the growth curve of their culture in sweat (Fig. S3), the *B. subtilis* population undergoes exponential growth until the nutrient is completely depleted even though the growth was not as much as in the standard nutrient-rich Luria Broth (LB) medium. Even with the protection from the skin microbiome and potential antibiotic substances available in sweat, *B. subtilis* grew well. The growth of skin microbiome was observed, but it was negligible compared to that of *B. subtilis* in sweat. We checked to see how well *B. subtilis* could grow in heat-treated sweat, which can destroy nutrients by direct thermal degradation. Bacterial growth was significantly minimized with the increase in temperature for the treatment (Fig. S3). In that sense, our skin, which maintains the temperature of 36 °C and keeps nutrients conserved, can be the excellent place for growth of the selected *B. subtilis*.

Although it is challenging to understand the effect of the inclusion of *B. subtilis* on the entire skin community, the study on the interaction between *B. subtilis* and the selected members of our skin bacteria can provide an enhanced understanding of *B. subtilis* on actual human skin and its commensal or competitive capabilities with other skin microorganisms. First, we studied the interaction between *B. subtilis* and *Staphylococcus capitis* (a skin-inhabiting bacterium). As shown in Fig. 5a, bacterial colonies of *B. subtilis* and *S. capitis* were spotted on an agar plate at very close proximity. A colony of *S. capitis* was placed on each side of the *B. subtilis* colony. After 24 h, each colony avoided competition and expanded. Even the larger colony of *B. subtilis* did not inhibit the growth of *S. capitis* showing commensal or mutualistic interaction. However,

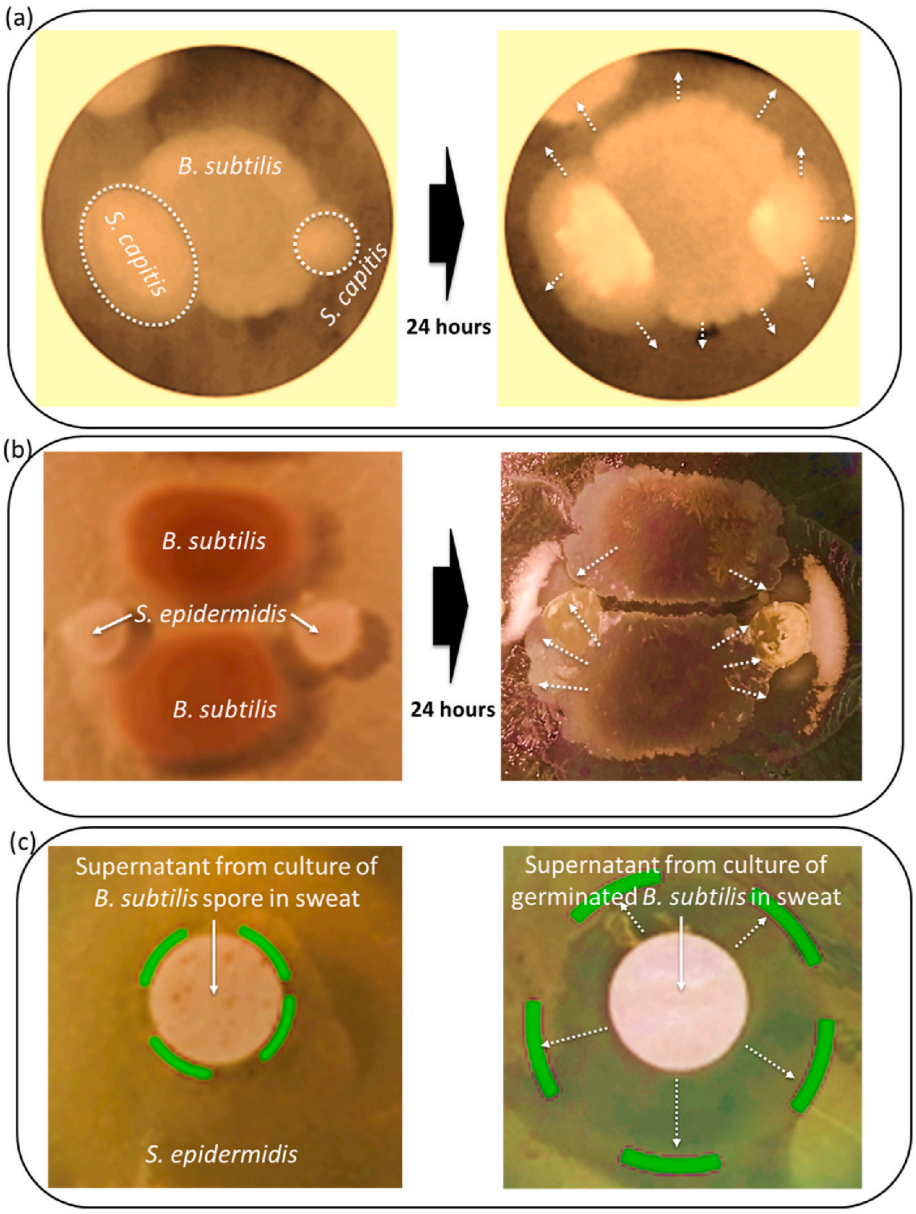

Fig. 5. Commensal and competitive interactions of *B. subtilis* with skin microorganisms. (a) commensal interaction with *S. capitis*, (b) competitive interaction with *S. epidermidis*, and (c) antibacterial susceptibility testing of overnight bacterial supernatants of *B. subtilis* spores and germinated *B. subtilis*.

when we chose a colony of *Staphylococcus epidermidis* (one of the most abundant skin bacteria) to assess its interaction with *B. subtilis*, a competitive interaction was observed. The colony of *B. subtilis* expanded, which inhibited the growth of the two colonies of *S. epidermidis* (Fig. 5b). This experiment is in good agreement with recent studies about how *B. subtilis* negatively affects the growth of *S. epidermidis* (Hernandez-Valdes et al., 2020; Moskovicz et al., 2021). They demonstrated that antibiotics produced from *B. subtilis* could inhibit the growth of *S. epidermidis*. Given that *S. epidermidis* is often regarded as easily adaptable and capable of becoming a pathogen (Hernandez-Valdes et al., 2020), the potential of *B. subtilis* to produce antibiotics can be beneficial to maintain the healthy skin microbial communities and avoid other bacterial invasions of the wearable devices. As shown in Fig. 5c, overnight bacterial supernatant from the germinated *B. subtilis* cultured in human sweat showed antibiotic effectiveness against the culture of *S. epidermidis* while the bacterial spores did not induce any antibiotic effects. While *B. subtilis* is known to produce several antibiotics, they can maintain this function even in sweat showing how this species can be effectively used for skin-mounted wearable applications.

3. Conclusion

This paper, *for the first time,* discovered *B. subtilis*' capability of (i) sporulation in the absence of sweat and limited availability of nutrients and (ii) germination in response to the presence of sweat without additional germinants. Furthermore, we generated on-demand energy by using the microbial metabolism of naturally secreted sweat and a long-term operational capability by allowing the cells to become dormant or zombie spores. This conceptual idea can support innovative sweat-based wearable applications working directly on the harsh environmental skin. *B. subtilis* can easily adapt to irregular and unpredictable perspiration as an on-demand biocatalyst responding to sweat availability. Although further studies will be needed to speed germination and to understand the long-term effect of *B. subtilis* on the skin microbiome and skin health, this work ensured the practical importance of the bacteria as a novel and sole sweat-activated catalyst for on-demand, long-lived wearable MFCs.

3.1. Experimental methods

Bacterial inoculum and sporulation *B. subtilis* was obtained from the American Type Culture Collection (ATCC) and was grown in 25 mL of LB medium overnight. Sporulation of *B. subtilis* was induced by using nutrient exhaustion in human sweat samples taken from three healthy volunteers. The sporulation and germination progressions were monitored with phase-contrast and fluorescence microscopy. For dormant spores, the cells have very low water contents and appear phase-bright with high refractive index. On the other hand, the germinating cells allow water uptake showing phase-dark with low refractive index. cFDA and PI dyes visualized the spore germination. The green cFDA uptake stains the metabolically active germinating cells while the red PI binds to the dormant spores and dead cells.

MFC fabrication A wearable MFC was fabricated on Whatman 3 MM chromatography paper, developing a flexible and cost-effective platform. The high porosity of paper allows for effective aeration and provides necessary gases for bacterial growth and sustaining cathodic reduction. The functional hydrophilic regions and the hydrophobic boundaries on paper were defined by wax printing with a Xerox Phaser Printer (ColorQube 8570). The MFC was constructed by using two functional paper layers: an anodic layer for bacteria inoculation and a cathodic reduction layer with an integrated wax-based membrane. The conductive anodic layer was engineered with the application of a poly (3,4-ethylenedioxythiophene):polystyrene sulfonate (PEDOT:PSS) and dimethyl sulfoxide (DMSO), followed by the addition of 3-glucidyloxypropyl-dimethoxysilane (GLYMO) for higher conductivity and hydrophilicity, respectively. The cathodic layer included a solid-state electron acceptor prepared with Ag_2O, and a wax-based membrane to electrically and ionically separate the anode and the cathode. The two functional layers were screen-printed with the graphite ink, and carefully assembled to form an MFC.

Electrical measurement setup The electrical performance of the MFC was assessed by measuring voltage drop across an external resistor using a data acquisition system (National Instruments, USB-6212). Every 30s, we recorded the drop through a LabView interface. The polarization curves and power outputs were obtained by the varied resistance method (1000, 500, 248, 68, 47, 22, 10, 5, 3.3, 2.2, 1.0, 0.5, 0.33, and 0.22 kΩ). Current densities and power densities were normalized to the total exposed anode area.

Commensal and competitive tests Commensal interaction of *B. subtilis* with *S. capitis* was performed on agar plates. A colony of *S. capitis* was spotted on each side of the relatively larger colony of *B. subtilis* in very close proximity. For the competitive interaction of *B. subtilis* with *S. epidermidis*, two small colonies of *S. epidermidis* were horizontally spotted between two large colonies of *B. subtilis* vertically placed. Unlike the commensal interaction test, the colonies were spotted at some distances without contact. The Kirby-Bauer disk-diffusion test was used for antibiotic susceptibility testing. A paper disk was impregnated with supernatants of *B. subtilis* cultures and placed on the agar plate grown overnight with *S. epidermidis* culture. If the paper disk contains antibiotics, an area of clear media where *S. epidermidis* are not able to grow surrounds the disk, which is known as the inhibition zone.

CRediT authorship contribution statement

Jihyun Ryu: Investigation, Methodology, Data curation. **Mya Landers:** Investigation, Formal analysis. **Seokheun Choi:** Conceptualization, Supervision, Project administration, Funding acquisition, Writing – original draft, Writing – review & editing, and finalization.

Declaration of competing interest

The authors declare that they have no known competing financial interests or personal relationships that could have appeared to influence the work reported in this paper.

Acknowledgments

This work was supported by the National Science Foundation (ECCS #1920979, #2020486 and #2100757) and the Office of Naval Research (#N00014-21-1-2412). We thank Prof. Ahyeon Koh for providing the integrated sweat simulator and the microfluidic interface.

Appendix A. Supplementary data

Supplementary data to this article can be found online at https://doi.org/10.1016/j.bios.2022.114128.

References

Baker, L.B., 2017. Sports Med. 47, S111–S128.
Barlya, M., Nyeln, H.Y.Y., Javey, A., 2018. Nat. Electron. 1, 160–171.
Brandwein, M., Steinberg, D., Meshner, S., 2016. npj Biofilms and Microbiomes 2, 3.
Byrd, A.L., Belkaid, Y., Segre, J.A., 2018. Nat. Rev. Microbiol. 16, 143.
Chen, S., Patil, S.A., Brown, R.K., Schroder, U., 2019. Appl. Energy 233–234, 15–28.
Choi, J., Ghaffari, R., Baker, L.B., Rogers, J.A., 2018. Sci. Adv. 4, eaar3921.
Christie, G., Setlow, P., 2020. Cell. Signal. 74, 109729.
Gao, Y., Choi, S., 2017. Adv. Mater. Technol. 2, 1600194.
Gao, Y., Choi, S., 2018. Adv. Mater. Technol. 3, 1800118.
Gao, Y., Mohammadifar, M., Choi, S., 2019. Adv. Mater. Technol. 4, 1970039.
Ghaffari, R., Rogers, J.A., Ray, T.R., 2021a. Sensor. Actuator. B Chem. 332, 129447.
Ghaffari, R., Yang, D.S., Kim, J., Mansour, A., Wright Jr., J.A., Model, J.B., Wright, D.E., Rogers, J.A., Ray, T.R., 2021b. ACS Sens. 6, 2787–2801.
Gray, D.A., Dugar, G., Gamba, P., Strahl, H., Jonker, M.J., Hamoen, L.W., 2019. Nat. Commun. 10, 890.

Hernandez-Rodriguez, J.F., Rojas, D., Escarpa, A., 2021. Anal. Chem. 93, 167–183.
Hernandez-Valdes, J.A., Zhou, L., de Vries, M.P., Kuipers, O.P., 2020. npj Biofilms Microbiomes 6, 30.
Ivanov, I., Vidakovic-Koch, T., Sundmacher, K., 2010. Energies 3, 803–846.
Jeerapan, I., Sempionatto, J.R., Wang, J., 2020. Adv. Funct. Mater. 30, 1906243.
Khanna, K., Lopez-Garrido, J., Pogliano, K., 2020. Annu. Rev. Microbiol. 74, 361–386.
Kong, L., Zhang, P., Wang, G., Yu, J., Setlow, P., Li, Y., 2011. Nat. Protoc. 6, 625.
Kumar, A., Hsu, L.H., Kavanagh, P., Barriere, F., Lens, P.N.L., Lapinsonniere, L., Lienhard, V.J.H., Schroder, U., Jiang, X., Leech, D., 2017. Nat. Rev. Chem. 1, 0024.
Liu, L., Mohammadifar, M., Elhadad, A., Tahernia, M., Zhang, Y., Zhao, W., Choi, S., 2021. Adv. Energy Mater. 11, 2100713.
Logan, B.E., Rossi, R., Ragab, A., Saikaly, P.E., 2019. Nat. Rev. Microbiol. 17, 307–319.
Manjakkal, L., Yin, L., Nathan, A., Wang, J., Dahiya, R., 2021. Adv. Mater. 33, 2100899.
Mohammadifar, M., Choi, S., 2017. Adv. Mater. Technol. 2, 1700127.
Mohammadifar, M., Tahernia, M., Yang, J.H., Koh, A., Choi, S., 2020. Nano Energy 75, 104994.
Mohammadifar, M., Zhang, J., Yazgan, I., Sadik, O., Choi, S., 2018. Renew. Energy 118, 695–700.
Moskovicz, V., Ben-El, R., Horev, G., Mizrahi, B., 2021. BMC Microbiol. 21, 231.
Nield, D., 2019. For the First Time, Bacteria Seen Entering Strange 'Zombie' Mode to Survive Starvation. Science alert. News article, Feb. 24.
Niu, Y., Liu, H., He, R., Li, Z., Ren, H., Gao, B., Guo, H., Genin, G.M., Xu, F., 2020. Mater. Today 41, 219–242.
Nyein, H.Y.Y., Bariya, M., Tran, B., Ahn, C.H., Brown, B.J., Ji, W., Davis, N., Javey, A., 2021. Nat. Commun. 12, 1823.
Oh, J., Byrd, A.L., Park, M., Kong, H.H., Segre, J.A., 2016. Cell 165, 854–866.
Osman, M.H., Shah, A.A., Walsh, F.C., 2010. Biosens. Bioelectron. 26, 953–963.
Osman, M.H., Shah, A.A., Walsh, F.C., 2011. Biosens. Bioelectron. 26, 3087–3102.
Pan, J.G., Kim, E., Yun, C., 2012. Trends Biotechnol. 30, 610–612.
Purohit, M., Sassi-Gaha, S., Rest, R.F., 2010. J. Microbiol. Methods 82, 282–287.
Rasmussen, M., Abdellaoui, S., Minteer, S.D., 2016. Biosens. Bioelectron. 76, 91–102.
Ryu, J., Choi, S., 2021. Biosens. Bioelectron. 186, 113293.
Sayer, C.V., Barat, B., Popham, D.L., 2019. PLoS One 14, e0218220.
Tahernia, M., Mohammadifar, M., Choi, S., 2020a. Micromachines 11, 99.
Tahernia, M., Mohammadifar, M., Gao, Y., Panmanee, W., Hassett, D.J., Choi, S., 2020b. Biosens. Bioelectron. 162, 112259.
Wu, H., Zhang, Y., Kjoniksen, A., Zhou, X., Zhou, X., 2021. Adv. Funct. Mater. 31, 2103976.
Xiao, X., Xia, H., Wu, R., Bai, L., Yan, L., Magner, E., Cosnier, S., Lojou, E., Zhu, Z., Liu, A., 2019. Chem. Rev. 119, 9509–9558.
Xu, Y., Fei, Q., Page, M., Zhao, G., Ling, Y., Stoll, S.B., Yan, Z., 2021. iScience 24, 102736.
Yang, Y., Gao, W., 2019. Chem. Soc. Rev. 48, 1465–1491.
Yeon, H., Lee, H., Kim, Y., Lee, D., Lee, Y., Lee, J., Shin, J., Choi, C., Kang, J., Suh, J.M., Kim, H., Kum, H., Lee, J., Kim, D., Ko, K., Ma, B.S., Lin, P., Han, S., Kim, S., Bae, S., Kim, T., Park, M., Loo, Y., Kim, E., Han, J., Kim, J., 2021. Sci. Adv. 7, eabg8459.
Zhang, X., Al-Dossary, A., Hussain, M., Setlow, P., Li, J., 2020. Appl. Environ. Microbiol. 86, 17.
Zhao, F.J., Bonmarin, M., Chen, Z.C., Larson, M., Fay, D., Runnoe, D., Heikenfeld, J., 2020. Lab Chip 20, 168–174.